

# High-pressure structural, elastic and electronic properties of the scintillator host material, $\text{KMgF}_3$

G. Vaitheeswaran<sup>1,\*</sup>, V. Kanchana<sup>1</sup>, R. S. Kumar<sup>2</sup>,

A. L. Cornelius<sup>2</sup>, M. F. Nicol<sup>2</sup>, A. Svane<sup>3</sup>, A. Delin<sup>1</sup> and B. Johansson<sup>1,4</sup>

<sup>1</sup>*Applied Materials Physics, Department of Materials Science and Engineering,  
Royal Institute of Technology, Brinellvägen 23, 100 44 Stockholm, Sweden*

<sup>2</sup>*High Pressure Science and Engineering Center and Department of Physics,  
University of Nevada, Las Vegas, Nevada 89154, USA*

<sup>3</sup>*Department of Physics and Astronomy,  
University of Aarhus, DK-8000 Aarhus C, Denmark*

<sup>4</sup>*Condensed Matter Theory Group, Department of Physics,  
Uppsala University, Box.530, SE-751 21, Uppsala, Sweden*

(Dated: October 30, 2018)

## Abstract

The high-pressure structural behaviour of the fluoroperovskite  $\text{KMgF}_3$  is investigated by theory and experiment. Density functional calculations were performed within the local density approximation and the generalized gradient approximation for exchange and correlation effects, as implemented within the full-potential linear muffin-tin orbital method. *In situ* high-pressure powder x-ray diffraction experiments were performed up to a maximum pressure of 40 GPa using synchrotron radiation. We find that the cubic  $Pm\bar{3}m$  crystal symmetry persists throughout the pressure range studied. The calculated ground state properties – the equilibrium lattice constant, bulk modulus and elastic constants – are in good agreement with experimental results. By analyzing the ratio between the bulk and shear moduli, we conclude that  $\text{KMgF}_3$  is brittle in nature. Under ambient conditions,  $\text{KMgF}_3$  is found to be an indirect gap insulator with the gap increasing under pressure.

## I. INTRODUCTION

KMgF<sub>3</sub> is a technologically important fluoro-perovskite. For example, it is used as a vacuum-ultraviolet-transparent (VUV-transparent) material for lenses in optical lithography steppers<sup>1</sup> and in electro-optical applications<sup>2,3</sup>. When doped with lanthanide ions, it is a very promising material for scintillators<sup>4</sup> and radiation dosimeters<sup>5,6</sup>. In addition the physical properties of KMgF<sub>3</sub> may have implications for understanding of the Earth's lower mantle<sup>7,8</sup>.

KMgF<sub>3</sub> was first synthesized by van Arkel<sup>9</sup> and has a simple cubic perovskite structure at room temperature<sup>10</sup>. KMgF<sub>3</sub> demonstrates great stability under high compression and has not been found to undergo any phase transition at any temperature or pressure, suggesting it may be used as an internal X-ray calibrant<sup>11</sup>.

Several experimental studies of the ground state properties of KMgF<sub>3</sub> have been performed. The elastic constants at ambient pressure have been measured by Rosenberg and Wigmore<sup>12</sup> and by Reshchikova,<sup>13</sup> while Jones investigated their pressure and temperature dependence<sup>14</sup>.

From the theoretical side, electronic structure calculations for KMgF<sub>3</sub> have been carried out by means of linear combination of atomic orbitals<sup>15</sup>, including the effects of doping with transition metal impurities in KMgF<sub>3</sub><sup>16</sup>. The electronic structures of divalent 3*d* transition metal impurities doped in KMgF<sub>3</sub> have been investigated by the pseudopotential method<sup>17</sup>, and the properties of vacancies were studied by Hartree-Fock cluster calculations<sup>18</sup>. The structural, electronic and optical properties of KMgF<sub>3</sub> were recently investigated by the full-potential linear augmented plane wave (FP-LAPW) method<sup>19</sup>.

The present work is a combined theoretical and experimental study of the ground state and high-pressure properties of KMgF<sub>3</sub>. We present the equation of state resulting from high-pressure diamond-anvil cell experiments on KMgF<sub>3</sub> up to 40 GPa. We also present the equation of state, the elastic constants and the electronic structure from theoretical calculations using two different approximations for the exchange-correlation functional.

The remainder of the paper is organized as follows. Details of the computational method as well as details of the experimental setup are outlined in section 2. The measured and calculated equations of state are presented in section 3 together with calculated ground state properties and elastic properties. The electronic structure and the pressure variation of the

band gap are discussed in section 4. Finally, conclusions are given in section 5.

## II. COMPUTATIONAL AND EXPERIMENTAL DETAILS

### A. The electronic structure method

The all-electron full-potential linear muffin tin orbital (FP-LMTO) method<sup>20</sup> is used to calculate the total energies and basic ground state properties of  $\text{KMgF}_3$  presented here. In this method, the crystal volume is split into two regions: non-overlapping muffin-tin spheres surrounding each atom and the interstitial region between the spheres. We used a double  $\kappa$  spdf LMTO basis (each radial function within the spheres is matched to a Hankel function in the interstitial region) to describe the valence bands. In the calculations we included the 3s, 3p, 4s, 4p, and 3d bases for potassium, the 3s, 2p, 3p, and 3d bases for magnesium, and the 2s and 2p bases for fluorine. The exchange correlation potential was calculated within the local density approximation (LDA)<sup>21</sup> as well as the generalized gradient approximation (GGA) scheme<sup>22</sup>. The charge density and potential inside the muffin-tin spheres were expanded in terms of spherical harmonics up to  $l_{max}=6$ , while in the interstitial region, they were expanded in plane waves, with 14146 waves (energy up to 156.30 Ry) included in the calculation. Total energies were calculated as a function of volume for a (16 16 16) k-mesh containing 165 k-points in the irreducible wedge of the Brillouin zone and were fitted to the Birch equation of state<sup>23</sup> to obtain the ground state properties.

The elastic constants were obtained from the variation of the total energy under volume-conserving strains, as outlined in Refs. 24 and 25.

### B. Experimental details

The high-pressure x-ray diffraction measurements used a sample of polycrystalline  $\text{KMgF}_3$  prepared by the solid state reaction method from high purity constituent materials as described elsewhere in several reports<sup>26,27,28</sup>. Diffraction patterns collected at ambient temperature and pressure showed a cubic ( $Pm\bar{3}m$ ) symmetry with a cell parameter  $a = 4.0060(2)$  Å for  $\text{KMgF}_3$  which closely agrees with earlier reports<sup>30,36</sup>. High pressures were generated by a Merrill-Bassett type diamond-anvil cell (DAC). An 185- $\mu\text{m}$  sample chamber was formed in a rhenium metal gasket with a pre-indentation of 60- $\mu\text{m}$  thickness. The powder sample

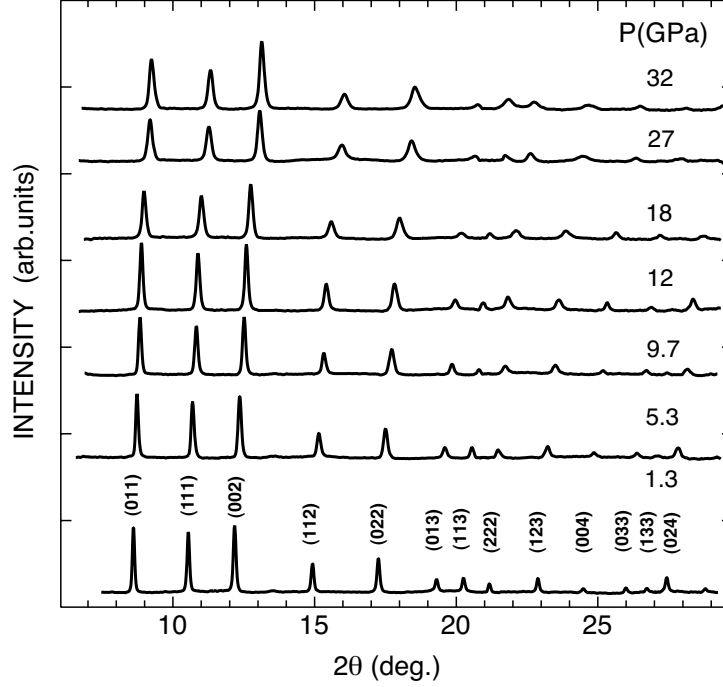


FIG. 1: Powder x-ray diffraction patterns recorded at various pressures up to 32 GPa. The indexing in terms of the simple cubic structure is given.

was loaded in the gasket with a few ruby grains and silicone fluid as pressure transmitting medium<sup>31</sup>. Diffraction experiments were performed at the 16ID-B undulator beam line of the High Pressure Collaborative Team (HPCAT) of the Advanced Photon Source (APS). A monochromatic x-ray beam with a wavelength of 0.4218 Å was focused down to a size of 30 x 30 μm. Diffraction images were collected with an image plate detector for an exposure time of 10 sec. The distance between the sample and the detector and the inclination angle of the image plate were calibrated using a CeO<sub>2</sub> standard.

The two dimensional images were subsequently integrated to one dimensional diffraction patterns using the Fit2D software<sup>32</sup>. The cell parameters were obtained by analyzing the diffraction patterns with the JADE software package and the P-V data obtained was fitted with a second-order Birch-Murnaghan<sup>23</sup> equation of state. The standard ruby fluorescence technique and the newly proposed ruby pressure scale of Holzapfel<sup>33</sup> were used to obtain the pressures in the sample chamber.

### III. GROUND STATE AND ELASTIC PROPERTIES

Powder x-ray diffraction patterns collected at several pressures are shown in Figure 1. On compression, the diffraction patterns remain unchanged up to 40 GPa, except for the shifts of diffraction lines caused by the decreasing lattice constant. This implies that no structural transformations occur up to 40 GPa in  $\text{KMgF}_3$ . Figure 2 shows the measured equation of state of  $\text{KMgF}_3$  and compares it with theoretical curves calculated within the LDA and GGA. The better theoretical description is obtained with the LDA which is somewhat surprising, since usually the GGA provides an improvement over LDA. At low pressures the LDA volume is slightly smaller than the experimental one, while the situation reverses at high pressures, *i. e.*, altogether the LDA predicts  $\text{KMgF}_3$  to be stiffer than experimental observations. GGA on the other hand greatly overestimates the equilibrium volume at ambient pressure, which is the main reason for the poor agreement with experiment. If the GGA curve is scaled throughout the pressure range with the error in equilibrium volume at  $P = 0$ , nearly perfect agreement is found with experiment (not shown).

The lattice constant and bulk modulus measured in the present work as well as values calculated within the LDA and GGA approximations are given in Table I. Results from earlier experimental and theoretical works are quoted for comparison. The bulk modulus obtained in our experiments  $B_0 = 71.2(2)$  GPa with  $B'_0 = 4.7(3)$  compares well with other experimental results listed in Table 1 and also with  $\text{NaMgF}_3$  reported recently by Liu et al<sup>37</sup> ( $B = 76.0(1.1)$  GPa). The lattice constant obtained within the LDA is 1.1 % lower than the experimental value, while the corresponding bulk modulus is 22% higher than the experimental value, which is the usual kind of accuracy of LDA. However the calculated LDA lattice constant from the present work agrees quite well with the experimental work when compared to the earlier FP-LAPW(LDA) calculations in which the reported lattice constant is 2.4% lower than the experimental value<sup>19</sup>. The LDA bulk modulus obtained from the present calculation agrees quite well the published FP-LAPW(LDA) results. When comparing the results obtained within GGA, the lattice constant is 1.9 % higher than the experimental value, whereas our results for the bulk modulus is within the spread of the experimental data. This truly excellent agreement regarding the bulk modulus is, however, a bit fortuitous. Since the calculated equilibrium volume is overestimated with GGA (and underestimated with LDA), an error – solely depending on the error in volume – is introduced

in the calculated bulk modulus. Therefore, we recalculated the bulk modulus also at the experimental volume in a manner similar to our earlier work<sup>38</sup> (see Table I). We find that this diminishes the discrepancies between the LDA and GGA results, as expected. In addition, the LDA bulk modulus now becomes *smaller* than the GGA one for  $\text{KMgF}_3$ , and both functionals are seen to actually overestimate the bulk modulus, by approximately 14 % (LDA) and 34 % (GGA).

The present experiments on  $\text{KMgF}_3$  relate to recent experiments performed for  $\text{NaMgF}_3$  and alloys of  $\text{NaMgF}_3$  and  $\text{KMgF}_3$ . The crystal chemistry of  $\text{Na}_{1-x}\text{K}_x\text{MgF}_3$  and  $\text{NaMgF}_3$  was studied in detail at ambient and at high pressures by Zhao et al.<sup>27,39</sup>.  $\text{NaMgF}_3$  undergoes a reversible phase transition from orthorhombic ( $Pbnm$ ) to tetragonal ( $P4/mbm$ ) and then to cubic structure ( $Pm\bar{3}m$ ) upon compression. These phase transitions require either compositional changes, by increasing the K concentration to 40%, or changing temperature or pressure. The structural changes in these perovskites are due to octahedral tiltings and shortening of Mg-F bonds compared to the cubic phase. A direct transformation from orthorhombic to cubic structure in  $\text{NaMgF}_3$ , however, requires a very high temperature (1038 K). Moreover, the transition temperature is reported to increase with pressure. The temperature dependence of the crystal structure of  $\text{KMgF}_3$  was recently investigated by neutron powder diffraction by Wood et al.<sup>11</sup> from 4.2 K to 1223 K, and the cubic symmetry was found to be stable throughout this temperature range. The thermal expansion as well as the atomic displacement parameters obtained in their experiments show that the F ions behave less anisotropically than in  $\text{NaMgF}_3$  at such high temperatures. On comparing these results with the present high-pressure diffraction experiments on  $\text{KMgF}_3$ , one may speculate that application of pressure alone would not be sufficient to induce structural changes in  $\text{KMgF}_3$  as the cubic phase is very stable. Such a phase transformation if any, would require either application of very high temperature or a composition change in the system to achieve changes in the order parameters. Asbrink et al.<sup>40</sup> have studied single crystals of the transition metal bearing perovskite  $\text{KMnF}_3$ , which is isostructural to  $\text{KMgF}_3$ , under high pressure and observed a cubic-to-tetragonal phase transition at a critical pressure of 3.1 GPa. On combining these results, phase transitions from the cubic symmetry may be expected with a combination of composition change, temperature and pressure in  $\text{KMgF}_3$ . A systematic study on the octahedral tilting and order parameters with other dopant compositions and the effect of external thermodynamical variables are further required to understand the phase

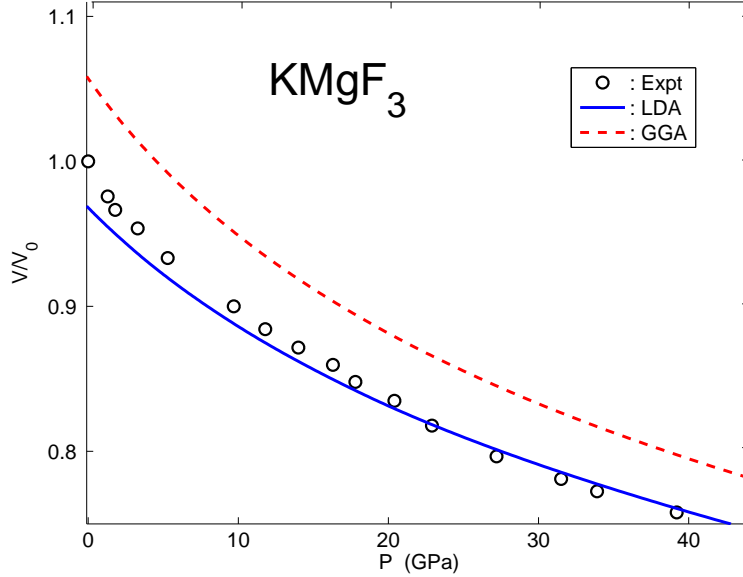


FIG. 2: (Color Online) Equation of state of  $\text{KMgF}_3$  in the pressure range from 0-40 GPa. The experimental datapoints are marked by circles, while theoretical results obtained with LDA and GGA are shown as full (blue) and dashed (red) curves. Volumes are given relative to the experimental equilibrium volume  $V_0 = 64.288 \text{ \AA}^3$ .

stability of  $\text{KMgF}_3$ .

The elastic constants of  $\text{KMgF}_3$  calculated within LDA and GGA are listed in Table 2 where they are also compared to experimental results as well as earlier calculations. The LDA overestimates all of the  $C_{11}$ ,  $C_{12}$  and  $C_{44}$  elastic constants by between 10% and 22% compared to experiment.<sup>12,13,14</sup> The elastic constants obtained within GGA are much closer to the experimental values than are the LDA results. For instance, both  $C_{11}$  and  $C_{12}$  are within the experimental spread. Of course, the elastic constants also depend sensitively on the volume, and, therefore, the same argument as for the bulk modulus can be applied here. We have, however, refrained from recalculating all the elastic constants with the volume correction, but wish to mention that the excellent agreement between experiment and the GGA elastic constants should be interpreted with care. Another point of caution is the fact that the calculated values pertain to 0 kelvin, while experiments are performed at room temperature. Finite temperature generally tends to reduce the elastic constants because of thermal expansion. Using the calculated elastic constants we calculated the anisotropy factor  $A = 2C_{44}/(C_{11} - C_{12})$ . We find an  $A = 0.91$  for LDA and  $A = 1.12$  for GGA.

The experimental result is 1.05, measured at room temperature<sup>12,13,14</sup>, which is closer to but lower than the GGA value. However, the anisotropy factor is found to decrease as the temperature is lowered<sup>13</sup>.

A simple relationship, which empirically links the plastic properties of materials with their elastic moduli was proposed by Pugh<sup>41</sup>. The shear modulus  $G$  represents the resistance to plastic deformation, while the bulk modulus  $B$  represents the resistance to fracture. A high  $B/G$  ratio is associated with ductility whereas a low value corresponds to brittle nature. The critical value which separates ductile and brittle materials is around 1.75, i.e. if  $B/G > 1.75$  the material behaves in a ductile manner, otherwise the material behaves in a brittle manner. Frantsevich<sup>42</sup>, in a similar fashion has suggested  $B/G \sim 2.67$  as the critical value separating brittle and ductile behavior. In the case of  $\text{KMgF}_3$  the calculated value of  $B/G$  is 1.5 within LDA and 1.4 within GGA, hence classifying this material as brittle.

Pettifor<sup>43</sup> suggested that the angular character of atomic bonding in metals and compounds, which also relates to the ductility, could be described by the Cauchy pressure  $C_{12} - C_{44}$ . For metallic bonding the Cauchy pressure is typically positive. On the other hand, for directional bonding with angular character, the Cauchy pressure is negative, with larger negative pressure representing a more directional character. These correlations have been verified for ductile materials such as Ni and Al that have typical metallic bonding, as well as for brittle semiconductors such as Si with directional bonding<sup>43</sup>. In the ionic compound  $\text{KMgF}_3$ , the calculated Cauchy pressure is -10 GPa within LDA and -15 GPa within GGA, in good agreement with the nonmetallic characteristics of  $\text{KMgF}_3$ .

Table 3 presents sound velocities as derived from the calculated elastic constants<sup>24</sup>. The calculated sound velocities agree quite well with the experiments, in particular for the GGA values, which is a consequence of the somewhat fortuitous good agreement between the measured and GGA calculated elastic constants.

#### IV. ELECTRONIC STRUCTURE

The calculated electron band structure of  $\text{KMgF}_3$  is shown in Figure 3 with the ensuing density of states in Figure 4. The valence bands consist of the F p bands with a gap of 7.24 eV to the conduction band, which is dominated by K states. The LDA bands are almost identical, however with a gap of only 6.95 eV. The gap increases almost linearly with



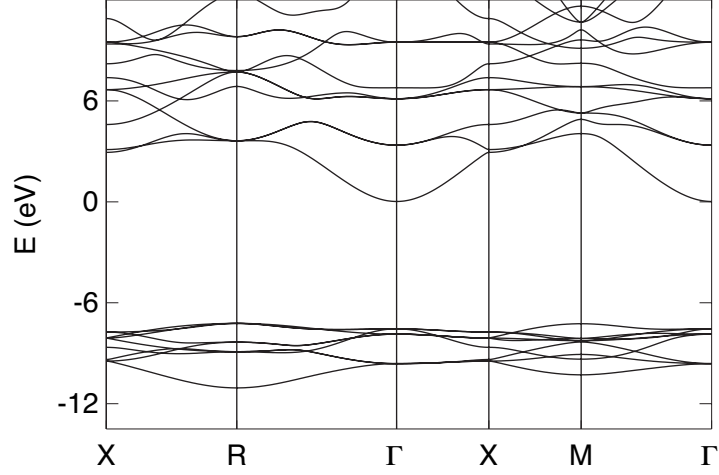


FIG. 3: Band structure of  $\text{KMgF}_3$  (using GGA, at the experimental lattice constant). The zero of energy is set at the position of the conduction band minimum.

compression, at the rate

$$V \frac{dE_g}{dV} = -7.1 \text{ eV}.$$

The conduction band minimum occurs at the  $\Gamma$  point, while the valence band maximum occurs at the R-point  $(1/2, 1/2, 1/2)\frac{2\pi}{a}$ . The largest occupied energy level at the M-point  $(1/2, 1/2, 0)\frac{2\pi}{a}$  is marginally lower (by  $\sim 0.02$  eV) than the valence band maximum at R, and it remains lower throughout the pressure range studied here.

## V. CONCLUSIONS

In conclusion, we find that pure cubic  $\text{KMgF}_3$  is very stable under high compression. From our analysis we also find that it is a brittle system and an indirect gap insulator whose gap increases with pressure

## Acknowledgments

G. V, V. K, A. D and B. J acknowledge VR and SSF for financial support and SNIC for providing computer time. One of the authors (R.S.K) is greatly indebted to his departed colleague Yongrong Shen for help in collecting the data. The authors gratefully acknowledge

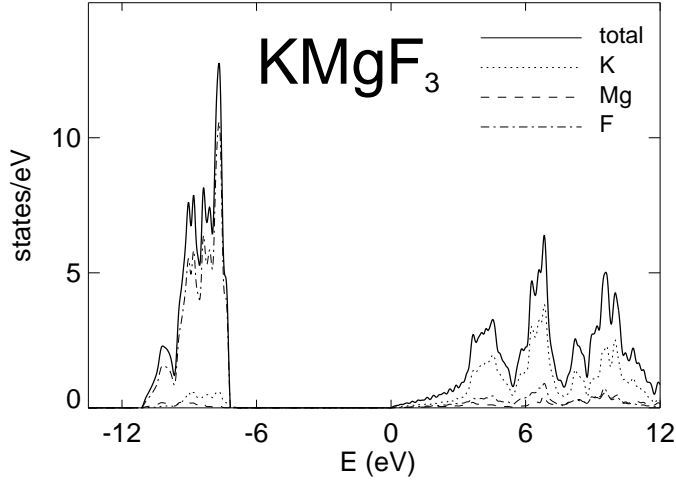


FIG. 4: Density of states of  $\text{KMgF}_3$  (using GGA, at the experimental lattice constant). The zero of energy is set at the position of the conduction band minimum. The partial projections onto the spheres of K, Mg and F are shown with dotted, dashed and dash-dotted lines, respectively, while full line gives the total density of states. Units are electrons per eV and per formula unit.

the use of the HPCAT facility supported by DOE-BES, DOE-NNSA, NSF, and the W. M. Keck Foundation. HPCAT is a high-pressure collaborative access team among the Carnegie Institution, Lawrence Livermore National Laboratory, the University of Nevada Las Vegas, and the Carnegie/DOE Alliance Center. We thank Dr. Maddury Somarazulu and other HPCAT staff for technical assistance. This research was supported from the U.S. Department of Energy Cooperative Agreement No. DE-FC52-06NA26274 with the University of Nevada Las Vegas.

TABLE I: Calculated lattice constants (in Å), Bulk modulus  $B_0$  (in GPa) and its pressure derivative  $B'_0$ , of KMgF<sub>3</sub> at the theoretical equilibrium volume compared with the experiment and other theoretical calculations. The bulk moduli have been calculated both at the experimental and theoretical volume ( $B_0(V_0^{\text{exp}})$  and  $B_0(V_0^{\text{th}})$ , respectively)

	Lattice constant	$B_0(V_0^{\text{th}})$	$B_0(V_0^{\text{exp}})$	$B'_0$
GGA <sup>a</sup>	4.0809	72.01	97.85	4.65
LDA <sup>a</sup>	3.9630	91.47	83.23	4.79
LDA, LAPW <sup>j</sup>	3.91	90.97	-	4.64
Expt.	4.0060(2) <sup>a</sup> , 3.973 <sup>b</sup> , 3.978±0.05 <sup>c</sup> , 3.9897 <sup>d</sup> , 3.993 <sup>e</sup> , 3.9839 <sup>f</sup>		71.2(2) <sup>a</sup> , 70.4 <sup>g</sup> , 75.1 <sup>h</sup> , 75.6 <sup>i</sup>	4.7(3) <sup>a</sup>

<sup>a</sup>Present work, <sup>b</sup>Ref.<sup>10</sup>, <sup>c</sup>Ref.<sup>34</sup>, <sup>d</sup>Ref.<sup>36</sup>, <sup>e</sup>Ref.<sup>35</sup>, <sup>f</sup>Ref.<sup>29</sup>, <sup>g</sup>Ref.<sup>12</sup>, <sup>h</sup>Ref.<sup>13</sup>, <sup>i</sup>Ref.<sup>14</sup> <sup>j</sup>Ref.<sup>19</sup>

TABLE II: Calculated elastic constants, shear modulus (G), and Young's modulus (E) all expressed in GPa, and Poisson's ratio  $\nu$  of KMgF<sub>3</sub> at the theoretical equilibrium volume

	$C_{11}$	$C_{12}$	$C_{44}$	G	E	$\nu$	
GGA	137.0	39.5	54.6	52.3	126.3	0.208	Present
LDA	177.0	48.7	58.7	60.9	149.5	0.228	Present
LDA	119.26	38.26	63.23	-	-	-	Ref. 19
Expt.	132±1.5	39.6±1.5	48.5±0.6	-	-	-	Ref. 12
	138±0.2	43.6±0.2	49.83±0.08	-	-	-	Ref. 13
	138.5±0.5	44.1±0.5	50.01±0.1	-	-	-	Ref. 14

TABLE III: Calculated longitudinal, shear, and average wave velocity ( $v_l$ ,  $v_s$ , and  $v_m$ , respectively) in m/s for  $\text{KMgF}_3$  at the theoretical equilibrium volume

		$v_l$	$v_s$	$v_m$
Present	LDA	7402	4396	4870
	GGA.	6706	4073	4507
Expt.		$6470^a, 6540^b$	$3940^a, 3900^b$	$4290^c$

<sup>a</sup>: Wave vector along  $\langle 100 \rangle$  direction, Ref.12, <sup>b</sup>: Wave vector along  $\langle 110 \rangle$  direction, Ref.12,

<sup>c</sup>: Ref.11

- 
- \* Author for Correspondence, E-mail: [vaithee@kth.se](mailto:vaithee@kth.se)
- <sup>1</sup> T. Nishimatsu, N. Terakubo, H. Mizuseki, Y. Kawazoe, D. A. Pawlak, K. Shimamura and T. Fukuda, *Jpn. J. Appl. Phys.* **41**, L365 (2002).
  - <sup>2</sup> G. Hörsch and H. J. Paus, *Opt. Commun.* **60**, 69 (1986).
  - <sup>3</sup> T. Fukuda, K. Shimamura, A. Yoshikawa, and E. G. Villora, *Opto-electron. Rev.* **9**, 109 (2001).
  - <sup>4</sup> P. Dorenbos, *Phys. Rev. B* **62**, 15640 (2000).
  - <sup>5</sup> A. V. Gektin, I. M. Krasovitskaya, and N. V. Shiran, *Radiat. Meas.* **29**, 337 (1998).
  - <sup>6</sup> C. Furetta, F. Santopietro, C. Sanipoli, and G. Kitis, *Appl. Radiation and Isotopes* **55**, 533 (2001).
  - <sup>7</sup> M. O’Keeffe and J.-O. Bovin, *Science* **206**, 599 (1979).
  - <sup>8</sup> J. N. Street, I. G. Wood, K. S. Knight, and G. D. Price, *J. Phys.: Condens. Matter*, **9**, L647 (1997).
  - <sup>9</sup> A. E. van Arkel, *Physica (Utrecht)* **5**, 166 (1925).
  - <sup>10</sup> H. Remy and F. Hansen, *Z. Anorg. Allg. Chem.* **283**, 277 (1956).
  - <sup>11</sup> I. G. Wood, K. S. Knight, G. D. Price and J. A. Stuart, *J. Appl. Cryst.* **35**, 291 (2002).
  - <sup>12</sup> H. M. Rosenberg and J. K. Wigmore, *Phys. Lett. A* **24**, 317 (1967).
  - <sup>13</sup> L. M. Reshchikova, *Soviet Physics-Solid State* **10**, 2019 (1969).
  - <sup>14</sup> L. E. A. Jones, *Phys. Chem. Minerals* **4**, 23 (1979).
  - <sup>15</sup> R. A. Heaton and C. C. Lin, *Phys. Rev. B* **25**, 3538 (1982).
  - <sup>16</sup> R. A. Heaton and C. C. Lin, *J. Phys. C* **18**, 3211 (1985).
  - <sup>17</sup> T. Nishimatsu, N. Terakubo, H. Mizuseki, Y. Kawazoe, D. A. Pawlak, K. Shimamura, N. Ichinose and T. Fukuda, *Jpn. J. Appl. Phys.* **42**, 5082 (2003).
  - <sup>18</sup> G. Q. Huang, L. F. Chen, M. Liu, and D. Y. Xing, *J. Phys.: Condens. Matter*, **15**, 4567 (2003).
  - <sup>19</sup> M. Sahnoun, M. Zbiri, C. Daul, R. Khenata, H. Baltache and M. Driz, *Mat. Chem. and Phys.* **91**, 185 (2005).
  - <sup>20</sup> S. Y. Savrasov, *Phys. Rev. B* **54**, 16470 (1996).
  - <sup>21</sup> S. H. Vosko, L. Wilk, and M. Nusair, *Can. J. Phys.* **58**, 1200 (1980).
  - <sup>22</sup> J. P. Perdew, K. Burke, and M. Ernzerhof, *Phys. Rev. Lett.* **77**, 3865 (1996).
  - <sup>23</sup> F. Birch, *J. Appl. Phys.* **9**, 279, (1938).

- <sup>24</sup> V. Kanchana, G. Vaitheeswaran, A. Svane and A. Delin, J. Phys.: Condens. Matter, **18**, 9615 (2006);
- <sup>25</sup> V. Kanchana, G. Vaitheeswaran and A. Svane J. Alloys and Compounds (2007), doi:10.1016/j.jallcom.2007.01.163
- <sup>26</sup> A. V. Chadwick, J. H. Strange, G. Ranieri, and M. Terenzi, Solid State Ion. **9-10**, 555 (1983).
- <sup>27</sup> Y. Zhao, J. Solid State Chem. **141**, 121 (1998).
- <sup>28</sup> R. W. Smith, W. N. Mei, J. W. Flocken, M. J. Dudik, and J. R. Hardy, Mat. Res. Bull. **35**, 341 (2000).
- <sup>29</sup> C. D. Martin, S. Chaudhuri, C. P. Grey and J. B. Parise, Amer. Mineral. **90**, 1522 (2005).
- <sup>30</sup> L. A. Muradyan, V. E. Zavodnik, I. P. Makarova, K. S. Aleksandrov, and V. I. Simonov, Kristallografiya **29**, 392 (1984).
- <sup>31</sup> Y. R. Shen, R. S. Kumar, M. Pravica, and M. F. Nicol, Rev. Sci. Instrum. **75**, 4450 (2004).
- <sup>32</sup> A. P. Hammersley, S. O. Svensson, M. Hanfland, A. N. Fitch, and D. Häusermann, High Pressure Res. **14**, 235 (1996).
- <sup>33</sup> W. B. Holzapfel, J. Appl. Phys. **93**, 1813 (2003).
- <sup>34</sup> A. Darabont, C. Neamtu, S. I. Fărcas, and G. Borodi, J. Crystal. Growth **169**, 89 (1996).
- <sup>35</sup> J. Lee, H. Shin, J. Lee, H. S. Chung, Q. W. Zhang, and F. Saito, Materials Transactions **44**, 1457 (2003).
- <sup>36</sup> A. R. Chakhmouradian, K. Ross, R. H. Mitchell, and I. Swainson, Phys. Chem. Minerals **28**, 277 (2001).
- <sup>37</sup> H. Z. Liu, J. Chen, J. Hu, C. D. Martin, D. J. Weidner, D. Häusermann, and H. K. Mao, Geophys. Res. Lett. **32**, L04304 (2005).
- <sup>38</sup> A. Delin, L. Fast, B. Johansson, O. Eriksson, and J. M. Wills, Phys. Rev. B **58**, 4345 (1998).
- <sup>39</sup> Y. S. Zhao, J. B. Parise, Y. B. Wang, K. Kusaba, M. T. Vaughan, D. J. Weidner, T. Kikegawa, J. Chen, and O. Shimomura, American Min. **79**, 615 (1994).
- <sup>40</sup> S. Asbrink, A. Waskowska, H. G. Krane, L. Gerward, and S. Olsen, J. Appl. Cryst. **32**, 174 (1999).
- <sup>41</sup> S. F. Pugh, Philos. Mag. **45**, 823 (1954).
- <sup>42</sup> I. N. Frantsevich, F. F. Voronov and S. A. Bokuta, *Elastic Constants and Elastic Moduli of Metals and Insulators Handbook*, edited by I. N. Frantsevich (Naukova Dumka, Kiev, 1983) pp. 60-180.

<sup>43</sup> D. Pettifor, *Mater. Sci. Tech.* **8**, 345 (1992).